ELSEVIER

Origin, Scaling, and Saturation of Second Order Polarizabilities in Donor/Acceptor Polyenes

Sergei Tretiak, Vladimir Chernyak, and Shaul Mukamel

Department of Chemistry, University of Rochester P. O. RC Box 270216 Rochester, NY 14627-0216

Abstract

Two-dimensional plots representing the changes in charge and bond-order distributions induced by the optical field are used to investigate the size-scaling of polarizabilities of donor/acceptor substituted elongated polyenes. The second order polarizability (β) is shown to originate from localized regions at the donor/acceptor ends and therefore saturates to a constant value, independent on polyene size n, for large n. In contrast, the linear (α) and cubic (γ) polarizabilities have contributions from the entire chain and grow linearly with n. These real-space plots reveal directly the relevant electronic coherence sizes that control the optical response and should be most valuable in the design of new optical materials.

I. INTRODUCTION

The connection between electronic structure and optical properties of organic compounds is an important fundamental problem [1] with numerous technological implications on optical materials and electroluminescent devices [2–4]. Polyenic oligomers are of particular interest as model systems of one-dimensional conjugated chromophores [5]. These molecules possess large optical polarizabilities due to delocalized π-electron excitations [4,6–8]. Adding an electron-withdrawing and an electron-donating group enhances the optical response even further [7,9–15]. The mechanisms leading to dramatic changes in optical polarizabilities with increasing chain length and donor/acceptor strength and the limiting factors of these enhancements are still not fully understood. Exploring the interplay between these two factors is a key for a rational design strategy of molecules

possessing large optical polarizabilities [2]. Experimental investigations are complicated by sample-quality, controlled synthesis and poor solubility of large molecules. On the theoretical side, different approaches are used for small molecules and bulk materials, making it hard to investigate the intermediate crossover regime.

The variation of off-resonant optical polarizabilities with molecular size may be described by the scaling law $\sim n^b$, n being the number of repeat units. In odd order responses (α, γ) the scaling exponents b vary considerably for short molecules: $1 < b_\alpha < 2$ and $2 < b_\gamma < 8$ depending on the system and model [6,16–19]. For elongated chains we expect the polarizability per repeat-unit α/n and γ/n to saturate and become size independent; The exponents b should thus attain the value 1, indicating that the polarizabilities become extensive properties. The saturation of γ/n was first predicted by Flytzanis and co-workers [18]. Recent theoretical studies indicate that it sets in at about 30-50 repeat units. A saturation length of ~ 200 was observed experimentally in one case [20].

Donor/acceptor substituted molecules possess even-order nonlinear polarizabilities. A comprehensive review of the current status of second order polarizability studies was given in [7]. Optical polarizabilities can be calculated using a perturbative expansion involving a summation over all molecular states. By restricting the summation to a single excited state and assuming that the charge-transfer transition is unidirectional, we obtain the two-level expression commonly used to estimate the second order polarizability

$$\beta \propto (\mu_{ee} - \mu_{gg})\frac{\mu_{ge}^2}{E_{ge}^2}, \qquad (1.1)$$

where μ_{gg} and μ_{ee} are the ground and excited state dipole

moments, μ_{ge} is the transition dipole, and E_{ge} is the transition frequency. It is not clear from Eq. (1.1) how should β scale with molecular size. Existing experimental and theoretical studies have not established the precise scaling law of β and its the crossover to the bulk. Experimental studies restricted by synthetic considerations to chain length of 11 repeat units show $1.4 < b_\beta < 3.2$ [7,9–12] whereas calculations performed with up to 22 repeat units yield $1.5 < b_\beta < 2$ [7,21]. Semiempirical calculations made by Morley suggest that for polyenes $b_\beta = 1$ [13,14] whereas for polyarenes $b_\beta = 0$ [15]. Using ($\beta/molecular\ volume$) as the figure of merit of different materials, he predicted that the optimal values in polyenic and polyarenic chromophores should be about 20 and 3 repeat units respectively [13–15].

In this paper we use a newly-developed Collective Electronic Oscillator (CEO) technique [22–24] which makes it possible to explore the variation of β over a broad size range, all the way to the bulk. Our calculations show that in marked contrast to α and γ, β itself (and not β/n) saturates for large sizes. We propose a real-space theoretical analysis that can readily account for this behavior, pinpoint the origin of β, and provide useful guidence for the synthesis of molecules with desirable nonlinear optical properties. Although the calculations presented here are for polyene bridges, this approach can be readily applied to a broad range of optical materials.

II. REAL-SPACE TWO-DIMENSIONAL ANALYSIS OF SUBSTITUTION EFFECTS

The present picture is based on the reduced single electron density matrix [25] which connects the optical polarizabilities directly to motions of charges in the molecule and totally avoids the calculation of excited electronic
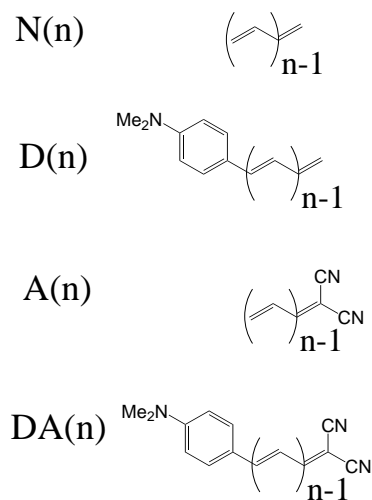

FIG. 1. Structures of the neutral $N(n)$, Donor $D(n)$, Acceptor $A(n)$, and Donor/Acceptor $DA(n)$ substituted molecules. Calculations were performed for bridges with $n =5,10,15,20,30,40$ double bonds.

eigenstates [22,23]. The density matrix offers an efficient computational scheme and provides a highly intuitive real-space physical picture for the optical response.

We consider a simplest model of a conjugated molecule where a single π orbital is located on each atom (i). The reduced single electron density matrix is defined as

$$\rho_{ij}(t) \equiv \langle\Psi(t)|c_i^+ c_j|\Psi(t)\rangle, \qquad (2.1)$$

where $|\Psi(t)\rangle$ is the many-electronic wavefunction of the molecule driven by the external field and $c_i^+ (c_i)$ are creation (annihilation) operators of an electron at the i'th atomic orbital. The diagonal elements ρ_{ii} represent the electronic π charge density at the i'th atom, whereas the off-diagonal elements, $i \neq j$, denote the bonding strength (i.e. bond order) between the two atoms [26–28]. The coherence size associated with the off-diagonal density matrix elements measures the degree of coherence between electrons at different sites, and controls, therefore, the scaling of molecular properties with size. The present coherence size is purely electronic in origin and reflects the loss of information when the many-electron density matrix is traced over all but one electrons. Nuclear motion and relaxation which are not included into the present calculations will contribute additional dephasing relaxation and will reduce the coherence size even further.

We calculated the optimal ground-state geometries of the donor/acceptor substituted polyenes shown in Fig. 1 at the AM1 level using Gaussian-94 [1]. The ZINDO code was then used to generate the INDO/S hamiltonian [29–31] and calculate Hartree-Fock ground-state density matrices $\bar{\rho}_{ij}$.

The effect of donor/acceptor substitutions on the chemical bonding pattern and charge distributions in the ground state can be visualized using contour plots of the density matrices in real-space [22,23]. Absolute values of the reduced single-electron ground-state density matrices elements $|\bar{\rho}_{ij}|$ of donor/acceptor substituted molecule DA(15) (n=15 is the number of double bonds) are shown in Fig. 2A. The axes represent carbon atoms of the bridge labeled 1-30 (In Figures 2 and 3 the donor end is labeled 1 and the acceptor end is $2n$). The density matrix is dominated by the diagonal and near-diagonal elements, reflecting the bonds between nearest neighbor atoms. The double bonds are clearly identified. To show the effect of substitution on the ground state we consider the difference matrix $\Delta\bar{\rho} \equiv |\bar{\rho}_{DA} - \bar{\rho}_N|$ between the density matrices of the substituted ($\bar{\rho}_{DA}$) and neutral (unsubstituted) ($\bar{\rho}_N$) molecules for various molecular sizes (see Fig. 1). The difference matrices for molecules with n=9, 15 and 30 are displayed in Fig. 3 A, B, and C respectively. These plots only show the polyenic bridge; The donor and the acceptor regions has been removed. For
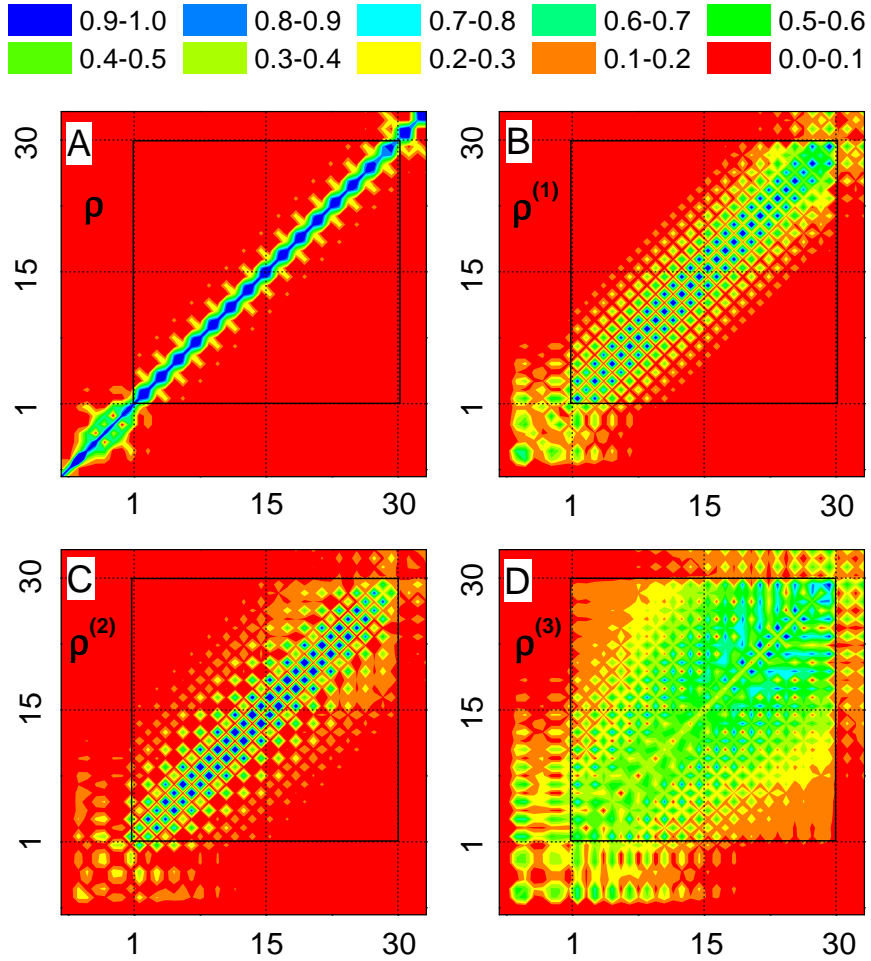

FIG. 2. Contour plots of the ground state density matrix $\bar{\rho}$ (**A**), and the density matrices induced by a static electric field $\delta\rho^{(1)}$ (**B**), $\delta\rho^{(2)}$ (**C**), and $\delta\rho^{(3)}$ (**D**) of molecule DA(15). The part of the density matrix corresponding to the bridge is marked by a rectangle. The axes are labeled by the bridge carbon atoms. Atom 1 (30) correspond to the donor (acceptor) ends.

clarity we magnified $\Delta\rho$ as indicated in each panel and used the same color code. The plots show that for large sizes (n=30 and 15) the donor and acceptor do not communicate directly and their effects are well confined to their respective vicinities; Consequently, the donor and the acceptor contributions to the dipole become additive. This is clearly illustrated in the top panel in Fig. 4 which shows that the ground-state dipole moment μ_{gg} of the donor/acceptor molecule is equal to the sum of dipole moments of molecules with donor only (D) and with acceptor only (A) substitutions. For shorter chains (e.g. $n = 9$ Fig. 3A) $\Delta\bar{\rho}$ is finite all across the chain, indicating a weak coupling of the donor and acceptor. The leveling off the ground-state dipole moments μ_{gg} of the donor/accceptor molecules with increasing of chain length (Fig. 4A) reflects the absence of long range electronic coherence in large polyenes and is crucial for predicting the scaling of optical properties with size, as will be shown below.

III. SIZE-SCALING OF OPTICAL POLARIZABILITIES

When the molecule is driven by an external field, its density matrix acquires a time-dependent part $\rho(t) = \bar{\rho} + \delta\rho(t)$. In the frequency domain we have [22,23]

$$\delta\rho_{ij}(\omega) = \delta\rho_{ij}^{(1)}(\omega) + \delta\rho_{ij}^{(2)}(\omega) + \delta\rho_{ij}^{(3)}(\omega) + \cdots. \quad (3.1)$$

where $\delta\rho_{ij}^{(k)}(\omega)$, the k'th order contribution in the incoming optical field, may be calculated by solving the time-dependent Hartree Fock(TDHF) equation of motion using the ground state density matrices as an input [22,23]. The k'th order polarizability is calculated by taking the expectation value of the dipole operator with respect to $\delta\rho^{(k)}(\omega)$. α, β, and γ are then calculated using $\delta\rho^{(1)}, \delta\rho^{(2)}$, and $\delta\rho^{(3)}$ induced by a static external field.

The resulting size-scaling of the off-resonant polarizabilities α/n, β and γ/n is depicted in Fig. 4, and the scaling exponents b_α, b_β and b_γ are displayed in Fig. 5. The behavior of b_α and b_γ which reach the value 1 at
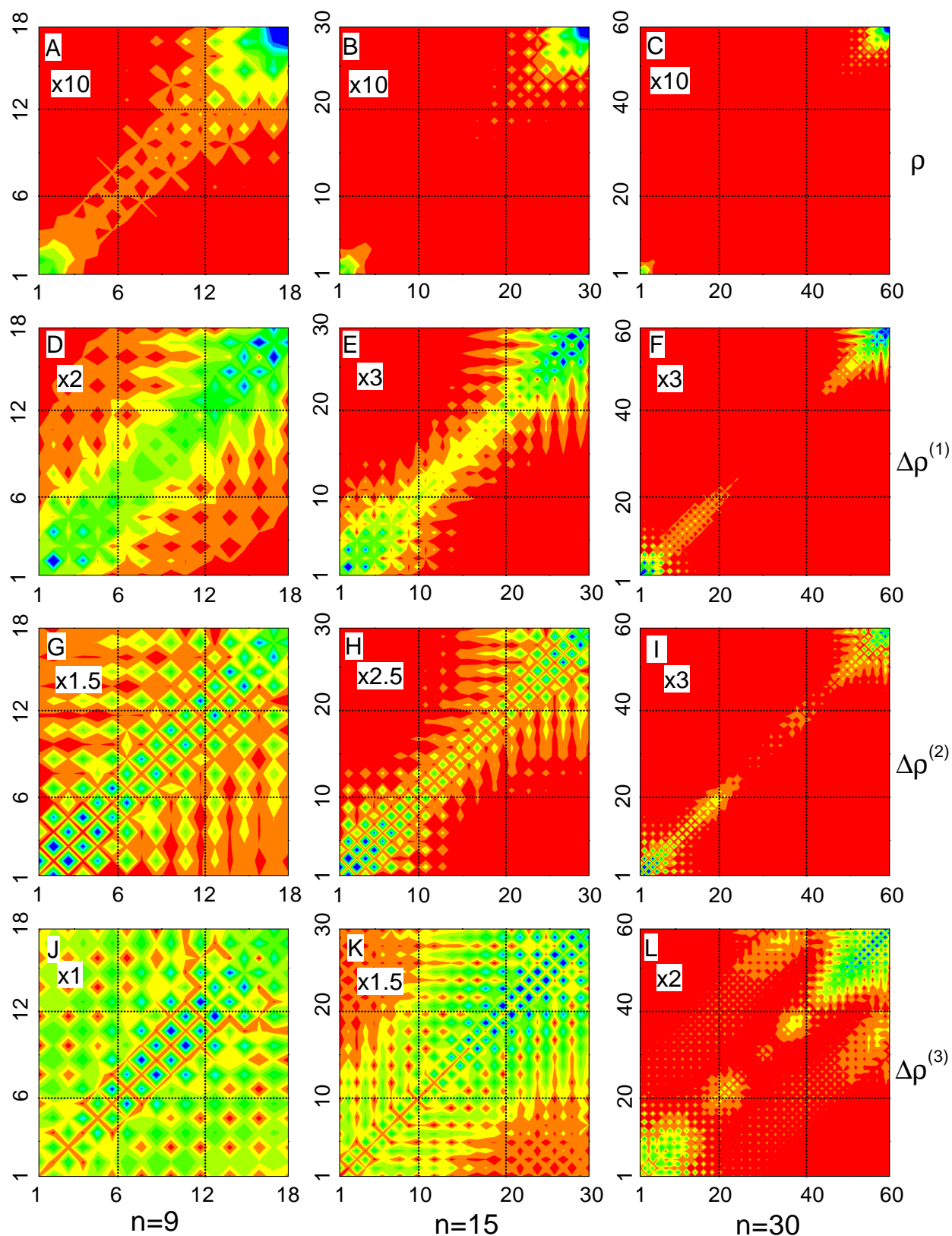
FIG. 3. Top row: Contour plots of the ground state difference matrices $\Delta\bar{\rho} = \bar{\rho}_{DA} - \bar{\rho}_N$ for n=9 (**A**), n=15 (**B**), and n=30 (**C**) shown for the bridge part of the matrix. Axes are labelled by the bridge carbon atoms with atom 1 on the donor side and atom 2n on the acceptor side. The second, the third, and the forth rows display the difference matrices to various orders in the field $\Delta\rho^{(1)}$, $\Delta\rho^{(2)}$, and $\Delta\rho^{(3)}$ respectively.

large sizes is consistent with the thermodynamic (bulk) limit. b_β, however is very different and vanishes at large sizes.

To visualize the optical response in real-space and analyze this markedly different behavior of β we examine the induced density matrices $\delta\rho^{(k)} = \delta\rho^{(k)}(\omega = 0)$ contributing to the optical response. In Fig. 2 we display the induced density matrix to first $\delta\rho^{(1)}$ (B), second $\delta\rho^{(2)}$ (C) and third $\delta\rho^{(3)}$ (D) order in the external field. Shown are the absolute magnitudes of these density matrices in the site representation, using the same format of the ground state calculations (Fig. 2A). These plots relate the optical properties directly to motions of charges in the sys-
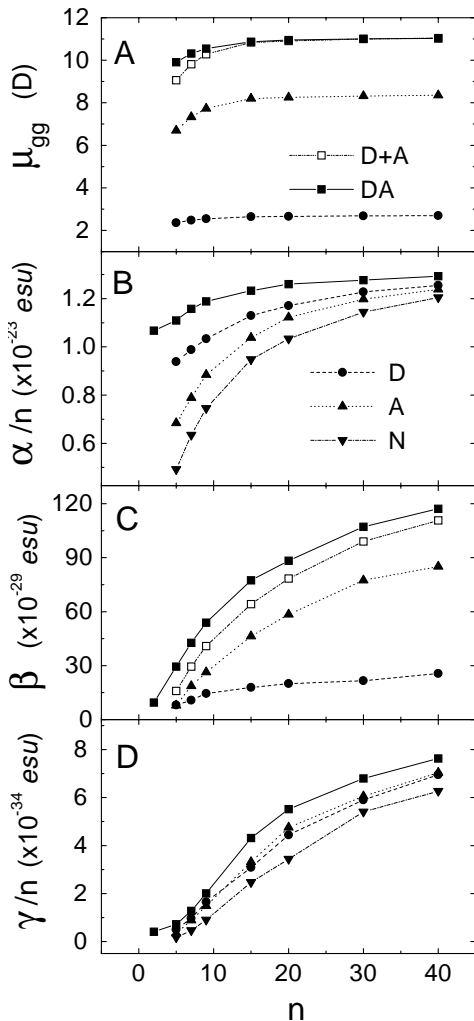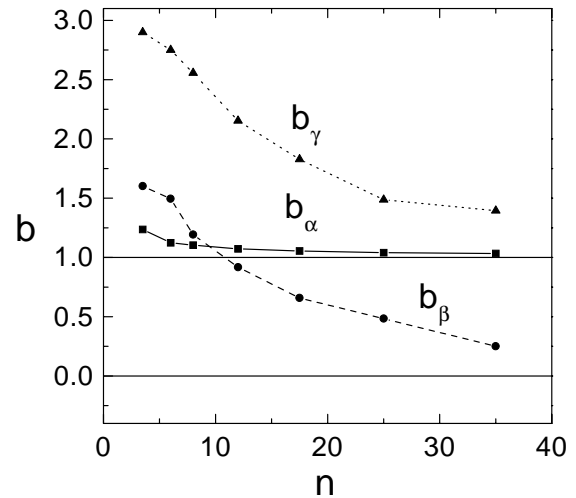

FIG. 5. Variation of the scaling exponents $b_\chi \equiv d[ln\ \chi]/d[ln\ n]$, $\chi = \alpha, \gamma, \delta$ with size for the curves shown in Fig. 4. At large sizes b_α and b_γ tend to 1 whereas b_β approaches 0. These reflect the saturation of $\alpha/n, \gamma/n$, and β shown in Fig. 4.

tem. The diagonal elements $\delta\rho_{jj}^{(k)}$ reflect induced charges on various atoms whereas the off-diagonal elements $\delta\rho_{ij}^{(k)}$ show the optically-induced coherences between i-th and j-th atomic orbitals. They may be viewed as dynamical bond-orders representing the joint amplitude of finding an electron on atom i and a hole on atom j. We note that the coherence size of the induced density matrix (given by its anti-diagonal section) increases as we move from panels B to D, indicating that higher nonlinearities induce a coherence between atoms farther and farther apart.

The effect of substitutions on the optical response can best be visualized by plotting the differences $\Delta\rho^{(k)} \equiv \delta\rho_{DA}^{(k)} - \delta\rho_N^{(k)}$ between the induced density matrices in the substituted and the neutral molecules. Because the neutral molecule does not possess quadratic polarizability, only the difference $\Delta\rho^{(2)}$ contributes to β. $\Delta\rho^{(1)}$, $\Delta\rho^{(2)}$, and $\Delta\rho^{(3)}$ are displayed at the second, third, and forth rows of Fig. 3 using the same format of the ground state calculations (top row). The most striking observation from these two-dimensional plots is that the donor/acceptor influence is screened by the π electrons and is confined to a finite section of the bridge with about 15-17 double bonds. For short chains (left column) the donor and acceptor communicate directly since their influence regions overlap spatially and significant electronic coherence develops between them. At large chains (n=30, right column) their effects are clearly separable. This is the reason why β levels off to a constant with $b_\beta = 0$: only the ends of the molecule contribute to β whereas the middle part is identical to that of neutral molecule with vanishing second order polarizability! This scaling is completely different from the behavior of α and γ; The entire molecule contributes to these odd order responses resulting in the fixed polarizability per unit molecular length at large sizes (Fig. 4B and D).

FIG. 4. Scaling with size and saturation of the ground state dipole moment μ_{gg} (**A**), the first (**B**), second (**C**), and third (**D**) orders off-resonant polarizabilities of the molecules displayed in Fig. 1. Neutral (no substitutions) N; acceptor substituted (A); • donor substituted (D); in panels **A** and **C** show the sum of molecules (A) and (D). The additivity of μ_{gg} and β at large sizes reflects the independent effect of the donor and acceptor. Note the similar saturation behavior of α/n, γ/n and β.

We can draw close analogy between size-scaling of the ground state dipole and the second order polarizability by comparing Fig. 3 with panels A and C of Fig. 4. Only limited coherence regions of the ground state density matrix and the induced density matrices at the molecular ends are affected by the donor and the acceptor. The size of these coherence regions depends on the donor and the acceptor strength. Both the ground state dipole moment and β saturate when the molecular size becomes larger than the size of these regions. For large chains the donor/acceptor contributions to the second order polarizability are additive, as illustrated in Fig. 4C: β of the donor/acceptor molecule (DA) becomes equal to the sum of β's of a molecule with only donor (D) and a molecule with only acceptor (A) substitutions. This additivity is similar to that displayed earlier for the permanent ground state dipole μ_{gg} (Fig. 4A).

Unlike the present real-space analysis, the mechanism of saturation of β at large sizes is highly nontrivial when examined using the molecular eigenstates (Eq. (1.1)). Since excited states are delocalized, we can argue that $\mu_{ge}^2 \sim n$ at large n in the two-level model [19,24]. This is necessary to guarantee that the linear scaling of the linear off-resonant polarizability with n: $\alpha \sim \frac{f_{ge}}{E_{ge}^2} = \frac{2\mu_{ge}^2}{E_{ge}} \sim n$, where f_{ge} is the oscillator strength. μ_{gg}, μ_{ee} and E_{ge} saturate with molecular size [9,10,13,14]. At first glance we thus expect $\beta \sim n$. This is however not the case, for the following reason: The difference $(\mu_{ee} - \mu_{gg})$ originates from charge redistribution upon electronic excitation. Fig. 3 clearly shows that charge transfer which affects the permanent dipole only occurs in confined regions at the ends. Since the excited states are delocalized over the entire molecule, the difference $(\mu_{ee} - \mu_{gg})$ should scale as n^{-1}, which cancels the $\sim n$ scaling of μ_{ge}^2, resulting in an overall constant β, independent of n. Another way to state this is that the ground state (μ_{gg}) and the excited state (μ_{ee}) contributions to β both scale as n, and the saturation of β originates from a delicate cancellation of these two $\sim n$ terms. It is interesting to note that similar cancellations have been observed in γ as well; Individual contributions which scale as n^2 interfere and almost cancel, resulting in the overall $\sim n$ scaling [32].

Defining and predicting the saturation size of optical properties has been the main focus of extensive theoretical effort [6,7]. This is a key factor in developing synthetic strategies for novel materials. The interference effects discussed above make it very difficult to predict trends using the molecular eigenstates. In contrast, our two-dimensional plots provide a highly intuitive yet quantitative tool for addressing this longstanding problem: the density matrix shows that the influence of the donor is limited to a few double bonds in its vicinity, and the same is true for the acceptor. The size of the influence region (along the diagonal and off-diagonal elements) in a large polyene defines the intrinsic coherence size of the system. When the molecular size is larger than the coherence size, the effects of the donor and the

acceptor are totally decoupled and additive; both β and μ_{gg} then become size-independent. This is reminiscent of the description of quantum confinement in semiconductor nanoparticles [33–35]. Our analysis shows that the donor and acceptor are decoupled even in an ideal chain when the purely-electronic response is calculated. Other factors such as vibrations and chain dislocations may contribute further to the decoupling of the donor and the acceptor, and the saturation may show up at shorter sizes.

The picture of electron transfer from donor to acceptor, accompanied by a giant dipole (and β) is therefore highly misleading in large polyenes. While direct donor-to acceptor charge transfer does occur at short chains, this is no longer the case for elongated molecules, as is evident from the lack of long-range electronic coherence between the donor and the acceptor.

ACKNOWLEDGMENTS

[1] M. Klessinger and J. Michl, *Excited States and Photochemistry of Organic Molecules*, VCH, New York (1995).

[2] S. R. Marder, B. Kippelen, A. K.- Y Jen, and N. Peyghambarian, *Nature*, **388**, 845 (1997).

[3] R. H. Friend, G. J. Denton, and H. F. Wittmann, *Solid State Communications*, **102**, 249 (1997).

[4] *Nonlinear Optical Properties of Organic Molecules and Crystals*, Vol. **1, 2**, J. Zyss and D. S. Chemla, Eds. (Academic Press, Florida, 1987).

[5] S. Speiser, *Chem. Rev.*, **96**, 1953 (1996).

[6] J. L. Brédas, C. Adant, P. Tackyx, A Persoons, and B. M. Pierce, *Chem. Rev.* **94**, 243 (1994).

[7] D. R. Kanis, M. A. Ratner, and T. J. Marks, *Chem. Rev.*, **94**, 195 (1994).

[8] S. R. Marder, W. E. Torruellas, M. Blanchard - Desce, V. Ricci, G. I. Stegeman, S. Gilmour, J. L. Brédas, J. Li, G. U. Bublitz, S. G. Boxer, *Science* **276**, 1233 (1997).

[9] M. Blanchard - Desce, C. Runser, A. Fort, M. Barzoukas, J.-M. Lehn, V. Bloy, V. Alain, *Chem. Phys.*, **199**, 253 (1995).

[10] M. Blanchard - Desce, R. Woltmann, S. Lebus, J.-M. Lehn, P. Kramer *Chem. Phys. Lett.*, **243**, 526 (1995).

[11] M. Blanchard - Desce, J.-M. Lehn, M. Barzoukas, C. Runser, A. Fort, G. Puccetti, I. Ledoux, and J. Zyss, *Nonlinear Optics*, **10**, 23 (1995).

[12] M. Blanchard - Desce, J.-M. Lehn, M. Barzoukas, I. Ledoux, and J. Zyss, *Chem. Phys.*, **181**, 281 (1994).

[13] J. O. Morley, *J. Chem. Soc. Perkins Trans.*, **II**, 1351 (1987).

[14] J. O. Morley, D. Pugh *Spec. Publ. - R. Soc. Chem*, **69**, 28 (1989).

[15] J. O. Morley, *J. Chem. Soc. Faraday Trans.*, **87**, 3009 (1991).

[16] J. F. Heflin, K. Y. Wong, Q. Zamani-Khamini, A. F. Garito, *Phys.Rev.B*, **38**, 1573 (1988).

[17] D. C. Rodenberger and A. F. Garito, *Nature* **359**, 309 (1992).

[18] G. P. Agrawal, C. Cojan, C. Flytzanis, *Phys.Rev.B*, **17**, 776 (1978).

[19] S. Tretiak, V. Chernyak, and S. Mukamel, *Phys. Rev. Lett.* **77**, 4656 (1996).

[20] I.D.W.Samuel, I.Ledoux, C.Dhenaut, J.Zyss, H.H.Fox, R.R.Schrock, R.J.Silbey, *Science* **265**, 1070 (1994).

[21] N. Matsuzawa, D. A. Dixon, *Int. J. Quantun Chemistry*, **44**, 497 (1992).

[22] S. Mukamel, S. Tretiak, T. Wagersreiter, and V. Chernyak, *Science*, **277**, (Aug. 8, 1997).

[23] V.Chernyak, S.Mukamel, *J.Chem.Phys.* **104**, 444 (1996).

[24] S. Tretiak, V. Chernyak and S. Mukamel, *J. Chem. Phys.*, **105**, 8914 (1996).

[25] E. R. Davidson, *Reduced Density Matrices in Quantum Chemistry* (Academic Press: New York, 1976).

[26] A. Szabo and N. S. Ostlund, *Modern Quantum Chemistry: Introduction to Advanced Electronic Structure Theory* (McGraw-Hill, New York, 1989).

[27] R. S. Milliken, *J.Chem.Phys.*, **23**, 1833, 1841, 2338, 2343, (1955).

[28] P. O. Lowdin, *Phys. Rev.* **97**, 1474, (1955); *Adv. in Phys.* **5**, 1, (1956).

[29] J. A. Pople D. L. Beveridge, and P. Dobosh, *J. Chem. Phys.*, **47**, 2026 (1967).

[30] J. Ridley and M. C. Zerner, *Theor. Chim. Acta*, **32**, 111 (1973).

[31] M. C. Zerner, G. H. Loew, R. F. Kirchner, and U. T. Mueller - Westerhoff, *J. Am. Chem. Soc.*, **102**, 589 (1980).

[32] S.Mukamel, *Principles of Nonlinear Optical Spectroscopy* (Oxford, New York, 1995).

[33] H. Haug and S. W. Koch, *Quantum Theory of the Optical and Electronic Properties of Semiconductors*, World Scientific, Singapore, 1994, 3rd ed.

[34] W. L. Wilson, P. S. Szajowski, and L. E. Brus, *Science* **262**, 1242 (1993).

[35] A. P. Alivisaros, *Science* **271**, 993 (1996).